3D Dynamics of Vortex Structures in a Quasi Two-dimensional Jet

Maxim V. Shestakov[1,*], Mikhail P. Tokarev[1], Dmitriy M. Markovich[1,2]

[1] Institute of Thermophysics, Siberian Branch of RAS, Novosibirsk, Russia
[2] Department of Physics, Novosibirsk State University, Novosibirsk, Russia
*corresponding author: mvsh@itp.nsc.ru

Abstract The work focuses on investigation of spatial-temporal 3D vortex structure of a quasi two-dimensional turbulent jet. Time-resolved tomographic PIV technique with repetition rate up to 10 kHz was used to measure 3D velocity distributions. It was shown that in quasi two-dimensional turbulent jet two types of coherent vortex structures exist. On the basis of instantaneous distributions of Q criterion 3D dynamics of vortex structure is studied. Longitudinal secondary vortex structures in far field of the quasi two-dimensional turbulent jet were detected for the first time.
Keywords: time-resolved tomographic PIV, quasi two-dimensional jet, dynamics of vortex structures

1 Introduction

The interest to quasi two-dimensional turbulent bounded jet flows is caused by wide variety of such flows in nature and industry, in particular because of presence of large-scale coherent vortex structures. Large-scale coherent vortex structures play important role in mixing and mass transfer, e.g. spread of contamination, momentum and energy transfer in shallow flows including rivers, lakes, channels and oceans.
Quasi two-dimensional turbulent jet flows are highly complex for numerical and experimental study. The complexity is determined by presence and interaction of disparate scales of turbulence. On the one hand this is three-dimensional small-scale turbulent motion of a scale h (thickness of fluid layer), on the other hand this is large-scale turbulent eddies induced by growth of shear instability in horizontal direction.
One of the first studies related to large-scale quasi two-dimensional vortex structures is [1]. In the work the structure of far field of quasi two-dimensional jet spreading in a narrow channel was studied in a wide range of channel depth values h. The authors emphasized two flow areas: near field of the jet (three-dimensional flow) where secondary flows have a great impact and far field of the jet (quasi two-dimensional flow), which is characterized by large-scale quasi two-dimensional vortices. The authors showed that beyond a distance of approximately ten times the depth of the bounded fluid layer the jet starts to meander around its axis. Large vortical structures develop with axes perpendicular to the bounding surfaces of the fluid layer. With increasing distance, the size of these structures increases by pairing. These features of the jet are associated with the development of quasi two-dimensional turbulence. By the present time, studies of large-scale quasi two-dimensional vortex structures and meandering effect have been resumed as evidenced by a number of numerical and experimental research works.
For historical reasons studies of near field and far field of quasi two-dimensional bounded jet were carried out independently and intended to different goals. Initial interest to study of bounded jets was determined by development of jet fluidics for space and defense industry [2-6]. These works referred to walls influence on a flow structure in near field of a jet and directed to development of jet flow control techniques. It was shown that in the wall bounded jet secondary flows appear in mixing layer. In the works [3,4] the model of secondary flows development was proposed on the basis of vortex filament re-orientation. Turbulent properties of secondary flows in bounded jets with different aspect ratio were studied in [5,6]. In [5] a spatial vortex structure was described based on visualization, which confirms assumptions from [3,4]. In the work [1] the near field of quasi two-dimensional jet flow is also partially studied and a secondary flow existence area was defined. In order to confirm hypothesis of secondary flow development [3,4] in the work [7] measurements of three velocity components in the flow volume were done in the near field by means Tomo-PIV technique. Analyzing instantaneous velocity fields in flow volume reconstructed from first 10 POD modes the authors managed to determine longitudinal vortices, which are responsible for secondary flow development. However, insufficient spatial and temporal resolution did not allow them to answer a number of questions concerning secondary flow formation and development.

The present work continues the previous one [7] and investigates vortex structures formation and development processes, interaction with walls and each other in a quasi two-dimensional turbulent jet.

2 Experimental setup

The experimental setup consisted of a closed hydrodynamic contour, including a tank, a pump, flow meter, and measurement section. The measurement section was a narrow channel formed by two plates made of organic glass (size: 307x270 mm^2, thickness: 20 mm), located at a distance h = 4 mm from each other. The data were acquired for the Reynolds numbers of $Re = hU_0/\nu = 20\ 000$, where U_0 is the bulk flow velocity. The flow was seeded with 50 μm polyamide particles. The rectangular/square nozzle without contraction was formed by two flat inserts placed between the glass plates (see Fig.1). The nozzle widths were d = 4, 10 mm. Twenty thousands of 3D velocity snapshots were obtained for each regime and were further used to calculate statistical flow characteristics. Measurements were carried out in three slightly overlapped zones at tree distances from the edge of the nozzle 4h, 12h and 20h.

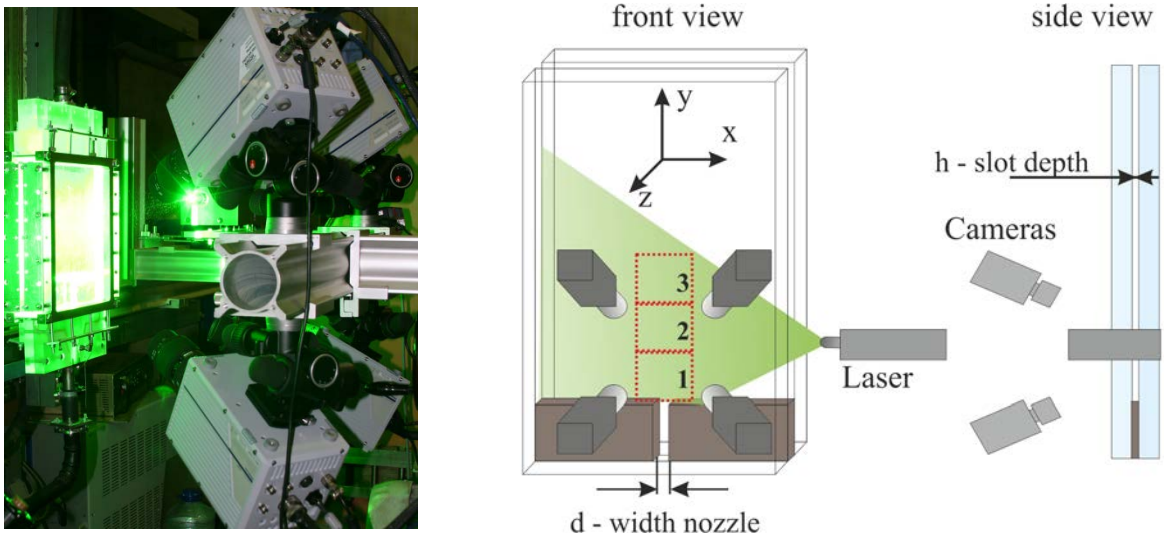

Fig. 1. Experimental setup for time-resolved Tomo-PIV measurements in a turbulent slot jet

The measurement system consisted of a high-repetition Nd: YAG laser (Photonix DM-532-150 DH with 15 mJ at 15 kHz), four high-speed CMOS cameras (Photron FASTCAM SA5 with resolution of 1024×1024 px of 12 bit images at 7 kHz), and synchronizing device Berkeley Nucleonics BNC 575. The thickness of the laser sheet was 4 mm. We used SIGMA AF 105 mm f/2.8 EX DG MACRO lenses for the optical setup. The size of the measurement area was 50×50 mm^2. We used three overlapped areas to cover the near, middle and far field of the jet. The frequency of particle image acquisition was 10 kHz, which corresponded to 100 us time interval between frames. For the first measurement volume three dimensional velocity fields were calculated using neighboring images, which corresponded to 10 kHz acquisition rate. For second and third measurement volume velocity field calculations were done using every second image, which corresponded to 5 kHz acquisition rate.

A precise Edmund Optics 50×50 mm^2 plane calibration target with a 1 mm step between reference circular markers was used. A precise traverse system was used to shift the cameras relative to the calibration target (fixed inside the slot) for the volumetric calibration. The cameras were equipped with 3D printed Scheimpflug adapters to align the focal plane to the sensor plane. We arranged the cameras in corners of a square with viewing angles equal to 30 degrees in the horizontal and vertical planes.

3 Data processing

We used home-made “ActualFlow” software to process the acquired data. A self-calibration procedure was done prior to the tomographic reconstruction. Also before the reconstruction step, the recorded projections were preprocessed by subtracting the minimum statistical intensity (for each pixel).

The size of a reconstructed 3D object was 615×615×70 voxels. The physical size of a voxel was approximately equal to 0.063×0.063×0.065 mm^3. The volume particle concentration was close to 8.5 particles per mm^3. The image density at this concentration upon the registered projections was 0.04 ppp. Self-calibration procedure was done to align all camera models directly using raw experimental particle images to get perfect multiple ray correspondence throughout the measurement volume. The maximum disparity was obtained at the level of two pixels. The residual disparity after three iterations of self-calibration procedure was below 0.02 pixels. For calibration parameter refinement self-calibration [8] using 300 images was done. The tomographic reconstruction was done by the implementation of the SMART and MENT [9] algorithms. Correlation analysis was performed using the iterative multigrid algorithm with continuous interrogation box shifting. The total number of iterations was four: two steps were performed with a resolution of 64×64×32 voxels and two extra iterations with a final resolution of 32×32×16 voxels. The grid-overlapping factor was set to 75%; therefore, the final correlation domain size for the calculation of a single velocity vector was 0.5×0.5×0.25 mm^3 with a half size distance between neighbor vectors.

4 Results and discussion

Preliminary results serving as a preface for the present work are shown in Fig 2. Fig.2 (top) shows vortices visualized by dye injection at the side edges of the jet in experimental setup described in [10]. Similar to work [1] two areas of the jet can be defined: near field and far field. The near field extending from the nozzle exit to x/h = 10 is characterized by constant expansion angle and intense entrainment of stagnant fluid to jet mixing layer, coherent vortex generation and secondary vortex presence. The far field is the area of two-dimensional turbulence, which is located after x/h = 10:14 and characterized by the formation of large-scale vortices and the presence of the meandering effect with periodic deviation from the axis of a flow. The meandering stream is adjacent to large two-dimensional vortex structures with the opposite sign of rotation, which increases with expansion of the jet.

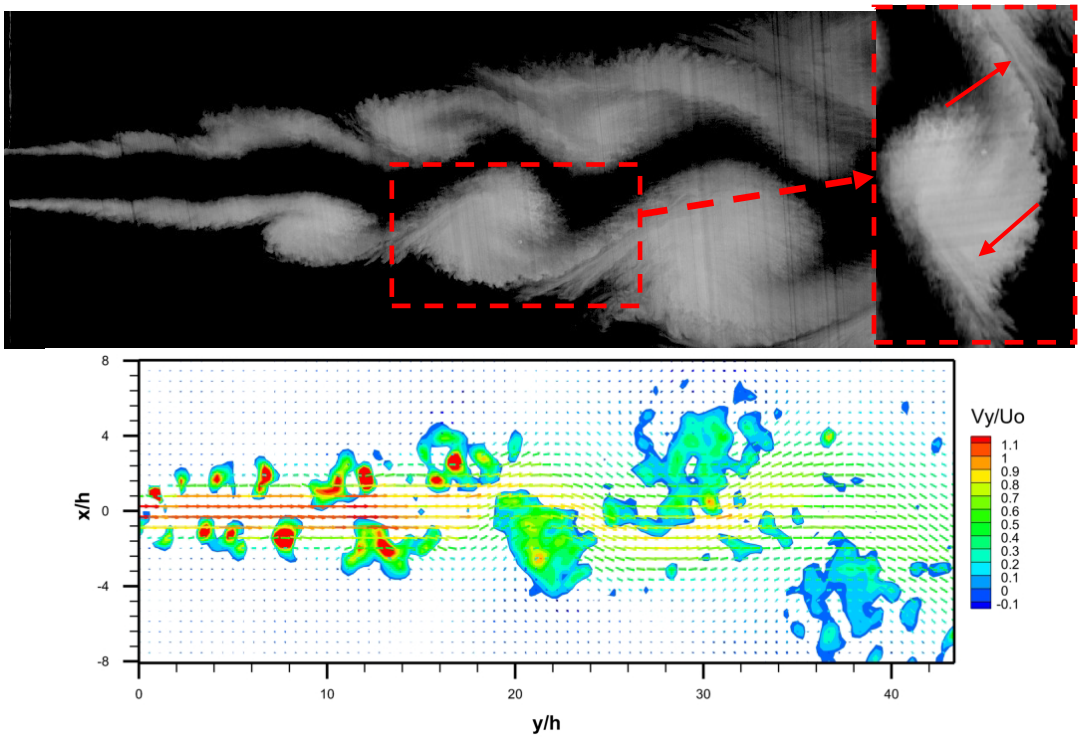

Fig. 2 Top. Dye visualization, experiment showing planar vortices Re=20 000, d/h = 10, h=2 mm frequency 8.4 kHz. Bottom. Velocity field and Q criteria in a middle plane. 2D PIV experiments. Re=20 000, d/h = 2.5, h=4 mm frequency 625 Hz [7]

Detailed analysis of dye visualization pictures showed that there are areas before and after the large-scale vortex structure where dye is distributed by means of longitudinal immiscible streaks (shown by red arrows). These thin structures before and after large scale vortex drew our attention and we carried out experiment using high speed tomographic PIV technique [11] in order to reveal their nature.

Fig.2 (bottom) shows an instantaneous velocity field and the distribution of positive values of Q criterion calculated from instantaneous velocity fields obtained by planar time-resolved PIV for a sequence of frames in the central section (z = 0) at the equal distance from the bounding walls [7]. One can easily see the areas of vortex localization and their development downstream the flow.
Fig.3 shows isosurfaces of Q^{3D} criterion for consecutive instantaneous velocity fields in flow volume obtained with 10 kHz frequency in near field of the jet. Color defines a value of streamwise vorticity component. Consecutive instantaneous velocity fields are presented in five different cross sections. Streamwise oriented paired structures in Q^{3D} criterion distribution shown by red and blue color indicate two counter-rotating longitudinal vortex structures.

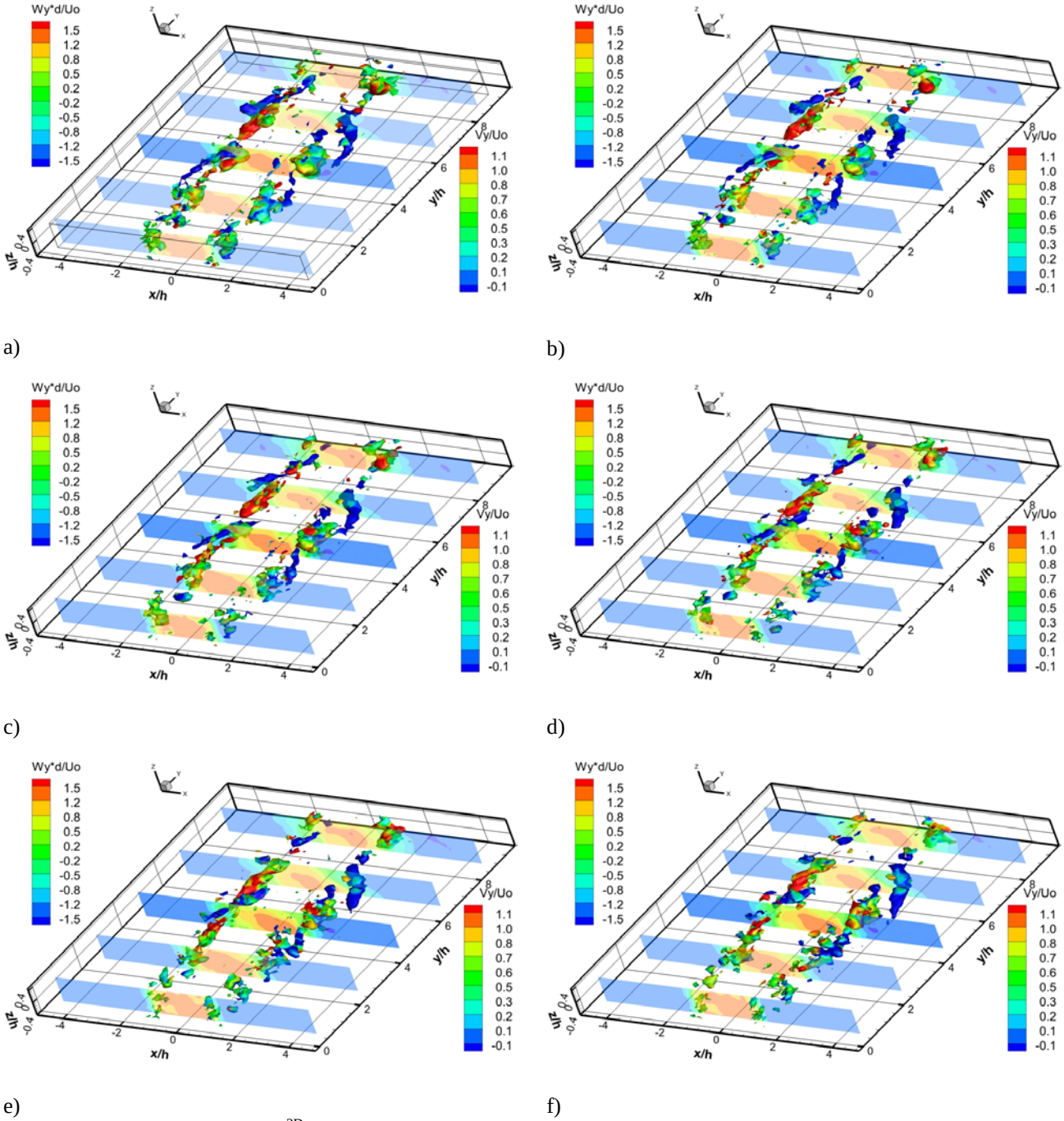

Fig. 3 Near field of the jet. Q^{3D} = 1.1 distribution. Consecutive velocity fields with time interval 100 us in between

One can see in Fig.3 a-f the evolution of longitudinal secondary vortex structures in the near field of the jet. These structures are formed in pairs as two counter-rotating vortices in jet mixing layer nearby bounding

walls. Paired vortex structures are generated because of their entrainment by the vortex structure arisen from Kelvin-Helmholtz instability. Downstream linear scale of secondary vortices increases due to pairing of co-directional longitudinal vortices. The presence of longitudinal secondary vortices in the near field of the jet leads to formation of secondary flows which were found in [3,4] for the first time. According to the work [1] secondary flows in quasi two-dimensional jet disappear at a distance of 10h. However our experiments showed the presence of secondary flows in far field of the jet which corresponds to >20h.
Fig.4 shows isosurfaces of Q^{3D} and Q^{2D} criteria. The color corresponds to streamwise vorticity component. Isosurfaces of Q^{2D} criterion covered by mesh were calculated using vx and vy velocity components in order to identify less intensive large scale quasi two-dimensional vortex structures. In five cross sections streamwise component of instantaneous velocity is presented. Fig. 4 a-f show consecutive isosurfaces of Q criterion calculated for each 14th instantaneous three-dimensional velocity field obtained with 5 kHz acquisition frequency. Time interval between shown pictures is 2.8 ms.

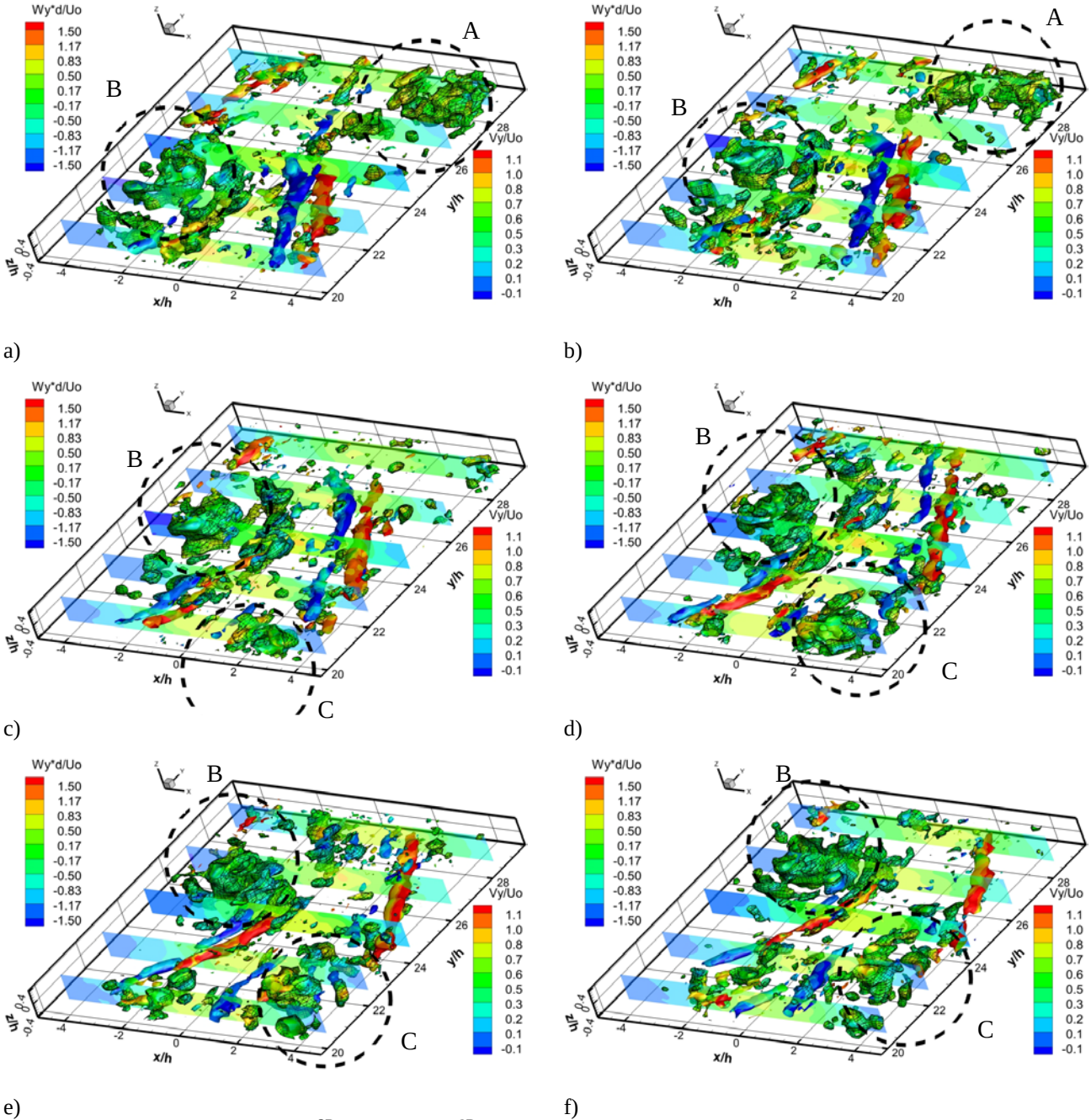

Fig. 4 Far field of the jet. Q^{3D} = 0.3 and Q^{2D} = 0.1 distribution. Every 14th frame (acquisition rate 5 kHz).

Analyzing Q criterion distribution pictures one can note that there are two types of coherent vortex structures in the flow: large-scale quasi two-dimensional vortex structures (L2DVS) marked by A, B, C letters and circles and secondary longitudinal vortex structures corresponding to isosurfaces colored with red and blue. L2DVS arranged in staggered order in the far field of the jet. Vortex structures are moving alternately left and right from the main jet flow. Similar dynamics of L2DVS was observed in works [1,7,10,12] and according to [14,15] it is driven by off-axis instability development.
Fig. 4 a-f show the far-field vortex structures and the dynamics of their interactions. Due to rotation of A vortex structure counter-rotating longitudinal secondary vortex structures are entrained to the core of the jet. As a result longitudinal secondary vortex structures become oriented in downstream direction and get into area of longitudinal stretching. While A vortex structure moves downstream the flow and B vortex structure develops, secondary vortices start to move from the core of the jet towards its boundary. In consequence of longitudinal vortex structure movement towards boundary of the jet, the vortex close to the jet core disappears while another one strengthens and continues to move towards jet boundary. Further development of B vortex structure downstream the flow leads to formation of paired counter-rotating longitudinal secondary vortex structures on another side of the jet. Interaction between B and C vortices causes strengthen of two counter-rotating longitudinal vortex structure in similar way as for A and B vortices. Consequent large-scale vortex structure interaction and jet meandering make longitudinal secondary vortex structures periodically being entrained into jet core and move toward jet boundary.
Fig. 5 shows isosurfaces of the streamwise component of the average velocity and cross-sections of the streamwise component of vorticity calculated using average velocity field for near field (a) and far field (b) of the jet. There is the area of secondary flows between core and boundary of the jet (Fig. 5 a) which shown by red and blue color for positive and negative values of streamwise vorticity correspondingly. Secondary flows are the consequence of longitudinal secondary vortex structure presence. There are secondary flows in far field of the jet (see Fig.5 b) which are less intensive in comparison with ones in near field of the jet. Their spatial structure is more complex and the area of influence is wider. Secondary flows in the far field are also due to longitudinal secondary vortex structures. However, one can see the direction of rotation of the secondary flows in the far field is opposite compared to the secondary flows in the near field of the jet. The difference in rotation directions in near field and far field of the jet is the subject for further analysis.

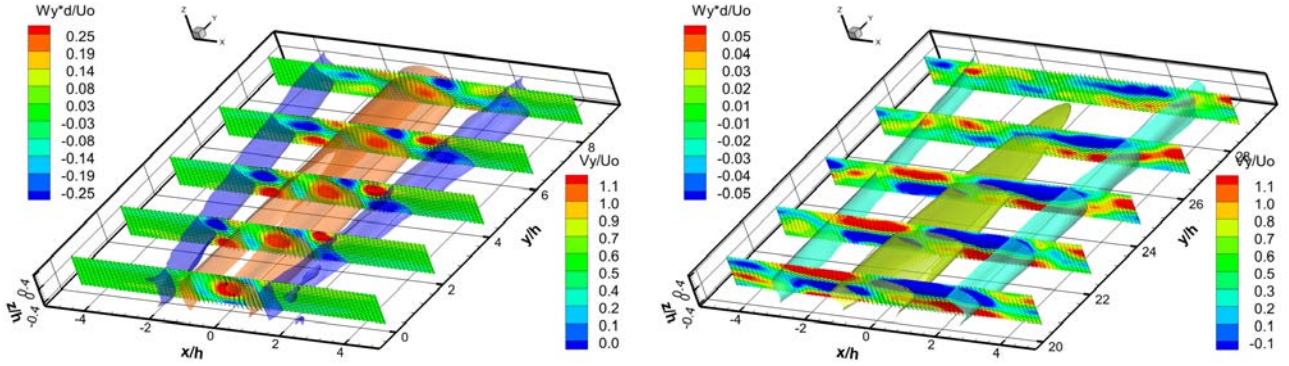

a) b)

Fig 5. a) Near and b) far field of the jet. Time-averaged 3D velocity data for a slot jet at d/h = 2.5 and Re = 2×10^4. Surfaces show constant values of the time-averaged streamwise velocity. Cross-sections denote streamwise vorticity of the average velocity.

5 Conclusions

We investigated the spatial-temporal 3D vortex structure of a quasi two-dimensional turbulent jet using the high-speed tomographic PIV technique. Velocity measurements were done for near field and far field of the jet. It was shown that in quasi two-dimensional turbulent jet two types of coherent vortex structures exist: large-scale quasi two-dimensional vortices and longitudinal secondary vortex structures. Experimental data analysis showed that longitudinal secondary vortex structures are formed in near field of the jet. Their linear scale increases downstream the flow. Longitudinal secondary vortex structures in far field of the quasi two-dimensional turbulent jet were detected for the first time.

6 Acknowledgements

This work is funded by President of Russian Federation via Leading Schools grant (NS-5984.2014.8) and Russian Foundation for Basic Research grant (No 14-08-31504 mol-a).

References

[1] Dracos, T, Giger, M, and Jirka, G (1992) Plane turbulent jets in a bounded fluid layer. *Journal of Fluid Mechanics*, vol. 241, pp. 587–614.

[2] McCabe, A., (1967) An experimental investigation of a plane subsonic jet with an aspect ratio of three. Proceeding of the Proceedings of the Institution of Mechanical Engineers vol. 183, pp. 342-346.

[3] Foss, J. F. & Jones J. B (1968) Secondary flow effects in a bounded rectangular jet. *Journal of Fluids Engineering*, vol. 90, pp. 241–248.

[4] Holdeman J., and Foss J. (1975) The initiation, development, and decay of secondary flow in a bounded jet. *Journal of Fluids Engineering*, vol. 97, pp. 342-352.

[5] Nozaki, T., et al., (1986) Experimental Study of a Bounded Jet Flow (Mechanism of the Secondary Flow), Proceeding of the 4th International Symp. Flow Visualization, pp.495-499.

[6] Nozaki, T., et al., , (1984) Study of a Bounded Jet Flow Considering the Initial Turbulence (Experiments with a Nozzle Having Aspect Ratio of 3), *Bull. Jpn. Soc. Mech. Eng*., vol.27, No.234, p.2730.

[7] Bilsky A.V., Markovich D.M., Shestakov M.V., Tokarev M.P. (2012) Tomographic PIV and planar Time-resolved PIV measurements in a turbulent slot jet // Proceeding of the 16th international symposium on applications of laser techniques to fluid mechanics, Lisbon.

[8] Wieneke, B., (2008) Volume self-calibration for 3D particle image velocimetry. *Experiments in Fluids*, vol. 45, pp. 549-456.

[9] Bilsky, A.V., Lozhkin, V.A., Markovich, D.M., and Tokarev, M.P. 2013. A maximum entropy reconstruction technique for tomographic particle image velocimetry. *Measurement Science and Technology*, vol. 24, 045301.

[10] Shestakov, M.V., Dulin, V.M., Tokarev, M.P., Sikovsky, D.P., and Markovich, D.M., 2014. PIV study of large-scale flow organisation in slot jets. *International Journal of Heat and Fluid Flow*, vol. 51, pp. 335-352.

[11] Scarano, F. 2013. Tomographic PIV: principles and practice. *Measurement Science and Technology*, vol. 24, 012001.

[12] Landel J. R., Caulfield C. P. and Woods A. W. (2012) Meandering due to large eddies and the statistically self-similar dynamics of quasi-two-dimensional jets *Journal Fluids of Mechanics*, vol. 692, pp. 347 368.

[13] Hunt, J.C.R., Wraya A.A., and Moin ,P. (1988) Eddies, stream, and convergence zones in turbulent flows. Center for Turbulence Research Report, CTR-S88, p. 193.

[14] Daoyi, C., and Jirka, G.H. (1998) Linear stability analysis of turbulent mixing layers and jets in shallow water layers. *Journal of Hydraulic Research*, Vol. 36, pp. 815-830.

[15] Jirka, G. H. (2001) Large scale flow structures and mixing processes in shallow flows. *Journal Hydraulic Research*, vol. 39, pp. 567–573.